NEUTRALINO PROTON CROSS SECTION AND DARK MATTER DETECTION

R. ARNOWITT, B. DUTTA AND Y. SANTOSO

Center For Theoretical Physics, Department of Physics, Texas A&M University, College Station TX 77843-4242, USA

We consider the neutralino proton cross section for detection of Milky Way dark matter for a number of supergravity models with gauge unification at the GUT scale: models with universal soft breaking (mSUGRA), models with nonuniversal soft breaking, and string inspired D-brane models. The parameter space examined includes $m_{1/2}$ <1 TeV and $\tan\beta < 50$, and the recent Higgs bound of m_h >114 GeV is imposed. (For grand unified models, this bound is to be imposed for all $\tan\beta$.) All coannihilation effects are included as well as the recent NLO corrections to $b \to s\gamma$ for large $\tan\beta$, and coannihilation effects are shown to be sensitive to A_0 for large $\tan\beta$. In all models, current detectors are sampling parts of the paramater space i. e. $\tan\beta \gtrsim 25$ for mSUGRA, $\tan\beta \gtrsim 7$ for nonuniversal models, and $\tan\beta \gtrsim 20$ for D-brane models. Future detectors should be able to cover almost the full parameter space for $\mu > 0$. For $\mu < 0$, cancellations can occur for $m_{1/2} \gtrsim 450$ GeV, allowing the cross sections to become $\lesssim 10^{-10}$ pb for limited ranges of $\tan\beta$. (The positions of these cancellations are seen to be sensitive to the value of $\sigma_{\pi N}$.) In this case, the gluino and squarks lie above 1 TeV, but still should be accessible to the LHC if $m_{1/2} < 1$ TeV.

1 Introduction

The existance of dark matter, which makes up about 30% of all the matter and energy in the universe, is well documented astronomically. However, what it is made of is unknown, and there have been many theoretical suggestions: wimps, axions, machos, etc. The Milky way consists of perhaps 90% dark matter, and so is a convenient "laboratory" for the study of dark matter, particularly by direct detection by terrestial detectors. We consider here the case of supersymmetric (SUSY) wimp dark matter and its detection by scattering by nuclear targets. In SUSY models with R-parity invariance, the wimp is almost always the lightest neutralino, $\tilde{\chi}_1^0$, and for heavy nuclei, the spin independent scattering dominates the cross section. Since then neutron and proton cross sections in the nuclei are nearly equal, it is possible to extract the $\tilde{\chi}_1^0 - p$ cross section, $\sigma_{\tilde{\chi}_1^0 - p}$, from any data (subject, of course, to astronomical uncertainties). Current detectors (DAMA, CDMS, UKDMC) are sensitive to cross sections

$$\sigma_{\tilde{\chi}_1^0 - p} \gtrsim 1 \times 10^{-6}\,\text{pb} \tag{1}$$

with perhaps an improvement on this by one or two orders of magnitude in the near future. More long range, future detectors (GENIUS, Cryoarray) plan on a significant increase in sensitivity, i.e. down to

$$\sigma_{\tilde{\chi}_1^0-p} \gtrsim (10^{-9} - 10^{-10})\,\text{pb} \tag{2}$$

We discuss here how such sensitivities might relate to what is expected from supersymmetry models.

We consider here three SUSY models based on grand unification of the gauge coupling constants at the GUT scale of $M_G \cong 2 \times 10^{16}$ GeV:

1. Minimal Supergravity GUT Models (mSUGRA)[1]. Here there are universal soft breaking masses occurring at scale M_G.

2. Non-universal Soft Breaking Models[2]. Here the first two generation of squarks and sleptons soft breaking masses are kept universal (to suppress flavor changing neutral currents) and the gaugino masses are universal at M_G, while nonuniversalities are allowed in the Higgs soft breaking masses and the third generation squark and sleptons masses at M_G.

3. D-brane String Models (based on type IIB Orientifolds)[3,4]. Here the $SU(2)_L$doublet scalar masses are different from the singlet masses at M_G, and the gaugino masses are similarly not degenerate.

The three types of models have varying amount of complexity in the soft breaking parameters, and while the first two models arise from natural phenomenological considerations in supergravity theory, there are also string models that can realise such soft breaking patterns. Though physically very different, all the models turn out to lead to qualitatively similar results: Current detectors are sensitive to a significant part of the SUSY parameter space, and future detectors should be able to cover most of the parameter space except for some special regions where accidental cancellations can occur which make $\sigma_{\tilde{\chi}_1^0-p}$ anomalously small. Thus dark matter experiments offer significant tests of supersymmetry over the same time scale (the next 5-10 years) that accelerator experiments will.

While each of the above models contain a number of unknown parameters, theories of this type can still make relevant predictions for two reasons: (i) they allow for radiative breaking of $SU(2) \times U(1)$ at the electroweak scale (giving a natural explanation of the Higgs mechanism), and (ii) along with calculating $\sigma_{\tilde{\chi}_1^0-p}$, the theory can calculate the relic density of $\tilde{\chi}_1^0$, i.e $\Omega_{\tilde{\chi}_1^0} = \rho_{\tilde{\chi}_1^0}/\rho_c$ where $\rho_{\tilde{\chi}_1^0}$ is the relic mass density of $\tilde{\chi}_1^0$ and $\rho_c = 3H_0^2/8\pi G_N$ (H_0 is the Hubble constant and G_N is the Newton constant). Both of these greatly

restrict the parameter space. In general one has $\Omega_{\tilde{\chi}_1^0} h^2 \sim (\int_0^{x_f} dx \langle \sigma_{\rm ann} v \rangle)^{-1}$ (where $\sigma_{\rm ann}$ is the neutralino annihilation cross section in the early universe, v is the relative velocity, $x_f = kT_f/m_{\tilde{\chi}_1^0}$, T_f is the freeze out temperature, $\langle ... \rangle$ means thermal average and $h = H_0/100$ km s^{-1}Mpc^{-1}). The fact that these conditions can naturally be satisfied for reasonable parts of the SUSY parameter space represents a significant success of the SUGRA models.

In the following we will assume $H_0 = (70 \pm 10)$km s^{-1}Mpc^{-1} and matter (m) and baryonic (b) relic densities of $\Omega_m = 0.3 \pm 0.1$ and $\Omega_b = 0.05$. Thus $\Omega_{\tilde{\chi}_1^0} h^2 = 0.12 \pm 0.05$. The calculations given below allow for a 2σ spread, i.e. we take [5]

$$0.02 \leq \Omega_{\tilde{\chi}_1^0} h^2 \leq 0.25. \tag{3}$$

It is clear that accurate determinations of the dark matter relic density will greatly strengthen the theoretical predictions, and already, analyses using combined data from the CMB, large scale structure, and supernovae data suggests that the correct value of the relic density lies in a relatively narrow band in the center of the region of Eq. (3)[6]. We will here, however, use the conservative range given in Eq. (3).

2 Theoretical Analysis

In order to get accurate predictions of the maximum and minimum cross sections for a given model, it is necessary to include a number of theoretical corrections. We list here the main ones: (i) In relating the theory at M_G to phenomena at the electroweak scale, the two loop gauge and one loop Yukawa renormalization group equations (RGE) are used, iterating to get a consistent SUSY spectrum. (ii) QCD RGE corrections are further included below the SUSY breaking scale for contributions involving light quarks. (iii) A careful analysis of the light Higgs mass m_h is necessary (including two loop and pole mass corrections) as the current LEP limits impact sensitively on the relic density analysis. (iv) L-R mixing terms are included in the sfermion (mass)^2 matrices since they produce important effects for large $\tan\beta$ in the third generation. (v) One loop corrections are included to m_b and m_τ which are again important for large $\tan\beta$. (vi) The experimental bounds on the $b \to s\gamma$ decay put significant constraints on the SUSY parameter space and theoretical calculations here include the leading order (LO) and NLO corrections. We have not in the following imposed $b - \tau$ (or $t - b - \tau$) Yukawa unification or proton decay constraints as these depend sensitively on unknown post-GUT physics. For example, such constraints do not naturally occur in the string models where $SU(5)$ (or $SO(10)$) gauge symmetry is broken by Wilson lines

at M_G (even though grand unification of the gauge coupling constants at M_G for such string models is still required).

All of the above corrections are now under theoretical control. In particular, the $b \to s\gamma$ SUSY NLO corrections for large $\tan\beta$ have recently been calculated [7,8]. We find that the NLO corrections give significant contributions for large $\tan\beta$ for $\mu > 0$. (We use here Isajet sign conventions for the μ parameter.) There have been a number of calculations of $\sigma_{\tilde{\chi}_1^0 - p}$ given in the literature [9,10,11,12,13,14,15], and we find we are in general numerical agreement in those regions of parameter space where the authors have taken into account the above corrections.

Accelerator bounds significantly limit the SUSY parameter space. As pointed out in [16], the LEP bounds on the Higgs mass has begun to make a significant impact on dark matter analyses. Since at this time it is unclear whether the recently observed LEP events [17] represent a Higgs discovery, we will use here the current LEP lower bound of 114 GeV [18]. There are still some remaining errors in the theoretical calculation of the Higgs mass, however, as well as uncertainty in the t-quark mass, and so we will conservatively assume here for the light Higgs (h) that $m_h > 110$ GeV for all $\tan\beta$. (For the MSSM, the Higgs mass constraint is significant only for $\tan\beta \lesssim 9$ (see e.g. Igo-Kemenes[18]) as Ah production with $m_A \cong m_Z$ can be confused with Zh production. However, in GUT models radiative breaking eliminates such regions of parameter space and the LEP constraint operates for all $\tan\beta$.) LEP data also produces a bound on the lightest chargino ($\tilde{\chi}_1^{\pm}$) of $m_{\tilde{\chi}_1^{\pm}} > 102$ GeV [19]. For $b \to s\gamma$ we assume an allowed range of 2σ from the CLEO data [20]:

$$1.8 \times 10^{-4} \leq B(B \to X_s\gamma) \leq 4.5 \times 10^{-4} \tag{4}$$

The Tevatron gives a bound of $m_{\tilde{g}} \geq 270$ GeV(for $m_{\tilde{q}} \cong m_{\tilde{g}}$)[21].

Theory allows one to calculate the $\tilde{\chi}_1^0$-quark cross section and we follow the analysis of [22] to convert this to $\tilde{\chi}_1^0 - p$ scattering. For this one needs the $\pi - N$ sigma term,

$$\sigma_{\pi N} = \frac{1}{2}(m_u + m_d)\langle p|\bar{u}u + \bar{d}d|p\rangle, \tag{5}$$

$\sigma_0 = \sigma_{\pi N} - (m_u + m_d)\langle p|\bar{s}s|p\rangle$ and the quark mass ratio $r = m_s/(1/2)(m_u + m_d)$. We use here $\sigma_0 = 30$ MeV [10], and $r = 24.4 \pm 1.5$[23]. Recent analyses, based on new $\pi - N$ scattering data gives $\sigma_{\pi N} \cong 65$ MeV[24,25]. Older $\pi - N$ data gave $\sigma_{\pi N} \cong 45$ MeV[26]. We will use in most of the analysis below the larger number. If the smaller number is used, it would have the overall effect in most of the parameter space of reducing $\tilde{\chi}_1^0 - p$ by about a

factor of 3. However, in the special situation for μ <0, where there is a cancellation of matrix elements, the choice of $\sigma_{\pi N}$ produces a more subtle effect, and we will exhibit there results from both values.

3 mSUGRA model

We consider first the mSUGRA model where the most complete analysis has been done. mSUGRA depends on four parameters and one sign: m_0 (universal scalar mass at M_G), $m_{1/2}$ (universal gaugino mass at M_G), A_0 (universal cubic soft breaking mass), $\tan\beta = \langle H_2\rangle/\langle H_1\rangle$ (where $\langle H_{(2,1)}\rangle$ gives rise to (up, down) quark masses) and $\mu/|\mu|$ (where μ is the Higgs mixing parameter in the superpotential, $W_\mu = \mu H_1 H_2$). One conventionally restricts the range of these parameters by "naturalness" conditions and in the following we assume $m_0 \leq 1$ TeV, $m_{1/2} \leq 1$ TeV (corresponding to $m_{\tilde{g}} \leq 2.5$ TeV, $m_{\tilde{\chi}^0_1} \leq 400$ GeV), $|A_0/m_{1/2}| \leq 4$, and $2 \leq \tan\beta \leq 50$. Large $\tan\beta$ is of interest since SO(10) models imply $\tan\beta \geq 40$ and also $\sigma_{\tilde{\chi}^0_1-p}$ increases with $\tan\beta$. $\sigma_{\tilde{\chi}^0_1-p}$ decreases with $m_{1/2}$ for large $m_{1/2}$.

The maximum value of $\sigma_{\tilde{\chi}^0_1-p}$ arises then for large $\tan\beta$ and small $m_{1/2}$. This can be seen in Fig.1 where $(\sigma_{\tilde{\chi}^0_1-p})_{\max}$ is plotted vs. $m_{\tilde{\chi}^0_1}$ for $\tan\beta$=20, 30, 40 and 50. Fig. 2 shows $\Omega_{\tilde{\chi}^0_1}h^2$ for $\tan\beta = 30$ when the cross section takes on its maximum value. Current detectors obeying Eq (1) are then sampling the parameter space for large $\tan\beta$, small $m_{\tilde{\chi}^0_1}$ and small $\Omega_{\tilde{\chi}^0_1}h^2$ i.e

$$\tan\beta \gtrsim 25,\ m_{\tilde{\chi}^0_1} \lesssim 90\text{GeV},\ \Omega_{\tilde{\chi}^0_1}h^2 \lesssim 0.1 \tag{6}$$

Further, as can be seen from Fig. 3, m_h does indeed exceed the current LEP bound over this entire region.

As discussed in [11], coannihilation effects in the early universe can significantly influence the relic density calculation. To discuss the minimum cross section, it is convenient then to consider first $m_{\tilde{\chi}^0_1} \lesssim 150$ GeV ($m_{1/2} \leq 350$) where no coannihilation occurs. The minimum cross section occurs for small $\tan\beta$. From Fig.4 one sees

$$\sigma_{\tilde{\chi}^0_1-p} \gtrsim 1\times 10^{-9}\text{pb};\ m_{\tilde{\chi}^0_1} \lesssim 140\text{GeV};\ \tan\beta = 6 \tag{7}$$

which would be accessible to detectors that are currently being planned (e.g. GENIUS).

For larger $m_{\tilde{\chi}^0_1}$, i.e. $m_{1/2} \gtrsim 350$ the phenomena of coannihilation can occur in the relic density analysis since the light stau, $\tilde{\tau}_1$, (and also $\tilde{e}_R$, $\tilde{\mu}_R$) can become degenerate with the $\tilde{\chi}^0_1$. The relic density constraint can then be

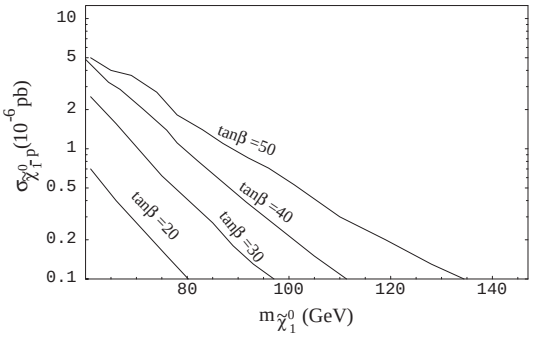

Figure 1. $(\sigma_{\tilde{\chi}^0_1-p})_{\max}$ for mSUGRA obtained by varying A_0 and m_0 over the parameter space for $\tan\beta = 20$, 30, 40, and 50[14]. The relic density constraint, Eq.(3) has been imposed.

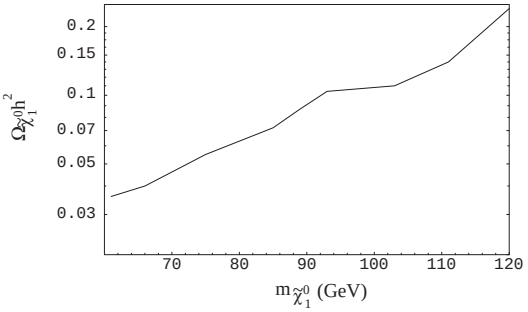

Figure 2. $\Omega_{\tilde{\chi}^0_1}h^2$ for mSUGRA when $(\sigma_{\tilde{\chi}^0_1-p})$ takes on its maximum value for $\tan\beta = 30$[14].

satisfied in narrow corridor of m_0 of width $\Delta m_0 \lesssim 25$ GeV, the value of m_0 increasing as $m_{1/2}$ increases and this was examined for low and intermediate $\tan\beta$ in [11]. Since m_0 and $m_{1/2}$ increase as one progresses up the corridor, $\sigma_{\tilde{\chi}^0_1-p}$ will generally decrease.

We consider first the case of $\mu > 0$ [27]. Coannihilation effects generally begin for $m_{1/2} \gtrsim 400$ GeV ($m_{\tilde{\chi}^0_1} \gtrsim 160$ GeV), and it is of interest to see what

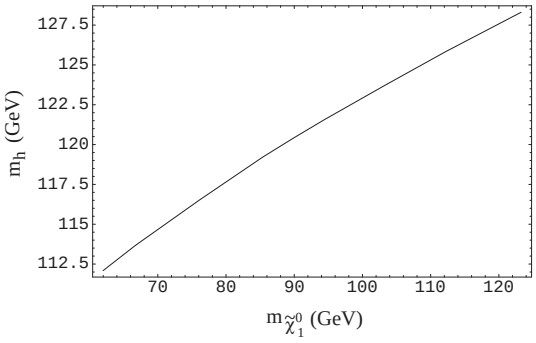

Figure 3. m_h for mSUGRA as a function of $m_{\tilde{\chi}_1^0}$ for $\tan\beta$ =30, when $\sigma_{\tilde{\chi}_1^0-p}$ takes on it maximum value[14].

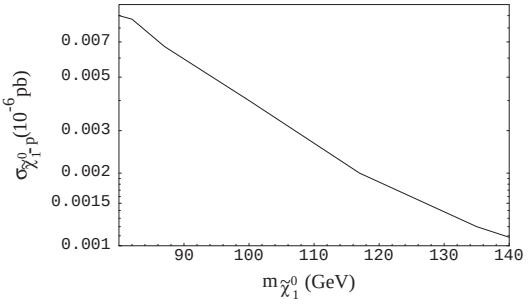

Figure 4. $(\sigma_{\tilde{\chi}_1^0-p})_{\rm min}$ for mSUGRA is plotted as a function of $m_{\tilde{\chi}_1^0}$ for $\mu >0$, $\tan\beta = 6$.

occurs for large $\tan\beta$. For large $\tan\beta$, there is only a coannihilation region left in the parameter space, and the allowed regions, exhibiting the allowed narrow corridors of parameter space are shown in Fig. 5 for $\tan\beta = 40$. In this domain the lightest stau ($\tilde{\tau}_1$) is the lightest slepton due to the large L-R mixing in the (mass^2) matrix, and so dominates the conanihilation effects. We note that the allowed corridors are sensitive to A_0, and large A_0 can allow large m_0 as $m_{1/2}$ increases. The thickness of the allowed corridors also decrease as A_0 increases. There is also a lower bound on $m_{1/2}$ for the allowed regions due to the $b \to s\gamma$ constraint, this bound decreasing with increasing A_0. (We note that this lower bound is sensitive to the NLO corrections discussed in Sec. 2 above.) Since larger A_0 allows for larger m_0 in the coannihilation region, the

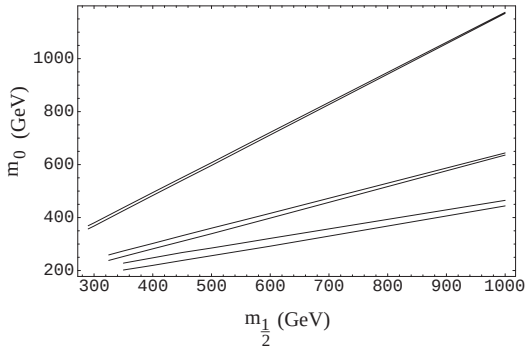

Figure 5. Allowed corridors for mSUGRA in the $m_0 - m_{1/2}$ plane satisfying the relic density constraint of Eq(3) for $\mu > 0$, $\tan\beta = 40$ (from bottom to top) $A_0 = m_{1/2}$, $2m_{1/2}$, $4m_{1/2}$ [27].

scattering cross section is a decreasing function of A_0. This is shown in Fig. 6 where $\sigma_{\tilde{\chi}_1^0 - p}$ is plotted as a function of $m_{1/2}$ for $\tan\beta = 40$ and $A_0 = 2m_{1/2}$, $4m_{1/2}$.

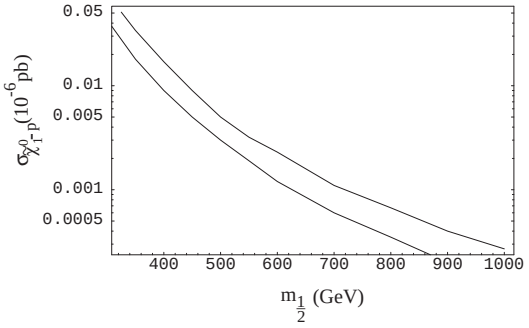

Figure 6. $\sigma_{\tilde{\chi}_1^0 - p}$ as a function of $m_{1/2}$ for mSUGRA, $\mu > 0$, $\tan\beta = 40$ and $A_0 = 2m_{1/2}$ (upper curve), $4m_{1/2}$ (lower curve).

We consider next $\mu < 0$. As discussed in [12], for low and intermediate $\tan\beta$, an accidental cancellation can occur in the heavy and light Higgs amplitudes in the coannihilation region which can greatly reduce $\sigma_{\tilde{\chi}_1^0 - p}$. We investigate here what happens at larger $\tan\beta$, and what is the domain over which this cancellation occurs. In Fig. 7 we have plotted $\sigma_{\tilde{\chi}_1^0 - p}$ in the large $m_{1/2}$ region,

for $\tan\beta = 6$ (short dash), 10(solid), 20(dot-dash), and 25(dashed). One sees that the cross section dips sharply for $\tan\beta = 10$, reaching a minimum at $m_{1/2} \simeq$725 GeV, and then rises. Similarly, for $\tan\beta = 20$, the minimum occurs at $m_{1/2} \simeq 830$ GeV while for $\tan\beta = 25$ at $m_{1/2} \simeq 950$ GeV. As a consequence, $\sigma_{\tilde{\chi}_1^0 - p}$ will fall below the sensitivity of planned future detectors for $m_{1/2}$ >450 GeV in a restricted region of $\tan\beta$, i.e.

$$\sigma_{\tilde{\chi}_1^0 - p} < 1 \times 10^{-10} \text{ for } 450\,\text{GeV} < m_{1/2} < 1\,\text{TeV};\ 5 \lesssim \tan\beta \lesssim 30;\ \mu < 0. \quad (8)$$

At the minima, the cross sections can become quite small, e.g. 1×10^{-13}pb, without major fine tuning of parameters, corresponding to almost total cancellation. Further, the widths of the minima at fixed $\tan\beta$ are fairly broad. While in this domain proposed detectors would not be able to observe Milky Way wimps, mSUGRA would imply that the squarks and gluinos then would lie above 1 TeV, but at masses that would still be accesible to the LHC. Also mSUGRA implies that this phenomena can occur only in a restricted range of $\tan\beta$, and for μ <0, so there would still be a number of cross checks of the theory.

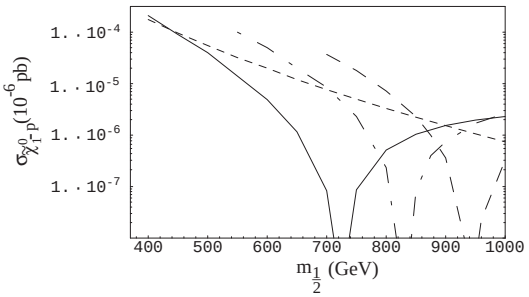

Figure 7. ($\sigma_{\tilde{\chi}_1^0 - p}$) for mSUGRA for $\mu < 0$, A_0 =1500 GeV for $\tan\beta = 6$ (short dash), 10 (solid), 20 (dot-dash), 25 (dashed). Note that the $\tan\beta = 6$ curve terminates at low $m_{1/2}$ due to the Higgs mass constraint, and the other curves terminate at low $m_{1/2}$ due to the $b \to s\gamma$ constraint.

In Sec. 2 it was pointed out that there was considerable uncertainty in the properties of the nucleon, particularly in the value of the $\sigma_{\pi N}$. In the above curves we have used $\sigma_{\pi N}$ =65 MeV. Fig. 8 gives a comparison for $\tan\beta = 10$ of this choice (solid curve) with the parameters of [12] (dashed curve) where $\sigma_{\pi N}$ =45 MeV is used. One sees that the position of the minimum at $m_{1/2}$ = 725 GeV is shifted to 600 GeV, with similar shifts occuring for the other values

of $\tan\beta$. Thus the cancellations ocurring in this region are quite sensitive to the properties of the proton.

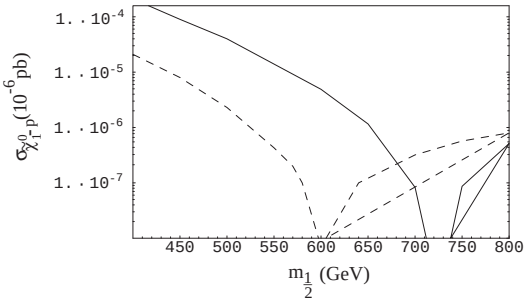

Figure 8. ($\sigma_{\tilde{\chi}_1^0-p}$) for mSUGRA for $\mu < 0$ $\tan\beta = 10$, $\sigma_{\pi N}$ =65 GeV (solid), and the parameters of [12] (dashed) where $\sigma_{\pi N}$ =45 GeV was used.

4 Nonuniversal SUGRA Models

In most discussions of SUGRA models with nonuniversal soft breaking terms, the universality of the the soft breaking masses at M_G of the first two generations of squarks and sleptons is maintained to suppress flavor changing neutral currents. However, one may allow both the Higgs masses and the third generation squark and slepton masses to become nonuniversal at M_G. One can parameterize this situation at M_G as follows:

$$\begin{aligned} m_{H_1}^2 &= m_0^2(1+\delta_1); \quad m_{H_2}^2 = m_0^2(1+\delta_2); \\ m_{q_L}^2 &= m_0^2(1+\delta_3); \quad m_{t_R}^2 = m_0^2(1+\delta_4); \quad m_{\tau_R}^2 = m_0^2(1+\delta_5); \\ m_{b_R}^2 &= m_0^2(1+\delta_6); \quad m_{l_L}^2 = m_0^2(1+\delta_7). \end{aligned} \tag{9}$$

where $q_L \equiv (\tilde{t}_L, \tilde{b}_L)$ squarks, $l_L \equiv (\tilde{\nu}_\tau, \tilde{\tau}_L)$ sleptons, etc. and m_0 is the universal mass for the first two generations of squarks and sleptons. The δ_i are the deviations from universality (and if one were to impose SU(5) or SO(10) symmetry one would have δ_3=δ_4= δ_5, and δ_6=δ_7.) In the following we limit the δ_i to obey:

$$-1 \leq \delta_i \leq +1 \tag{10}$$

and maintain gauge coupling constant unification and gaugino mass unification at M_G.

While there are a large numbers of new parameters, one can get an understanding of what effect they produce from the following. The neutralino $\tilde{\chi}_1^0$ is a mixture of gaugino (mostly Bino) and higgsino parts:

$$\tilde{\chi}_1^0 = \alpha\tilde{W}_3 + \beta\tilde{B} + \gamma\tilde{H}_1 + \delta\tilde{H}_2 \tag{11}$$

The dominant spin independent $\sigma_{\tilde{\chi}_1^0-p}$ cross section is proportional to the interference between the gaugino and higgino amplitudes, and this interference is largely governed by the size of μ^2. As μ^2 decreases, the interference increases, and hence $\sigma_{\tilde{\chi}_1^0-p}$ increases. Radiative breaking of $SU(2) \times U(1)$ determines the value of μ^2 at the electroweak scale. To see the general nature of the effects of nonuniverality, we consider low and intermediate $\tan\beta$ where an analytic form exists for μ^2 (see e.g. Arnowitt and Nath [2]):

$$\mu^2 = \frac{t^2}{t^2-1}\left[(\frac{1-3D_0}{2} - \frac{1}{t^2}) + \frac{1-D_0}{2}(\delta_3+\delta_4) - \frac{1+D_0}{2}(\delta_2 + \frac{\delta_1}{t^2})\right] m_0^2 + \text{universal parts} + \text{loop corrections}. \tag{12}$$

Here $t = \tan\beta$ and $D_0 \cong 1 - (m_t/200\text{GeV}\sin\beta)^2 \leq 0.2$ (Note that the Higgs and squark nonuniversalties enter coherrently, roughly in the combination $\delta_3 + \delta_4 - \delta_2$.) We see from Eq.(12) that μ^2 is reduced, and hence $\sigma_{\tilde{\chi}_1^0-p}$ increased for δ_3, δ_4, $\delta_1 < 0$, $\delta_2 > 0$, and μ^2 is increased for δ_3, δ_4, $\delta_1 > 0$, $\delta_2 < 0$. Thus one can get significantly larger cross sections in the nonuniversal models with the first choice of signs for the δ_i, and one can reduce the cross sections (though not by such a large amount) with the second choice. In general this would allow one to significantly lower the value of $\tan\beta$ from the rquirement of $\tan\beta \gtrsim 25$ for mSUGRA to come within the range of current detectors. The matter is complicated, however, by the experimental Higgs mass constraint (that $m_h > 110$) since theoretically the Higgs mass is small for low $\tan\beta$. We find, however, that one can reduce $\tan\beta$ to 7, and still maintain $m_h > 110$ GeV. This is exhibited in Fig. 9, where the maximum cross section is plotted as a function of $m_{\tilde{\chi}_1^0}$. The nonuniversal cross sections can be a factor of 10 or more greater than the corresponding universal ones allowing for these much lower values of $\tan\beta$.

As in mSUGRA, the minimum cross sections occur for the largest $m_{1/2}$ and smallest $\tan\beta$, and so they occur in the coannihilation region. We consider here the case where only the Higgs masses are nonuniversal i.e. $\delta_{1,2} \neq 0$ (the other δ_i set to zero). Results then are similar to the mSUGRA case. For $\mu > 0$ we find

$$\sigma_{\tilde{\chi}_1^0-p} \gtrsim 0.3(1) \times 10^{-10}\text{pb}; \text{ for } m_{1/2} \leq 1(0.6)\,\text{TeV} \tag{13}$$

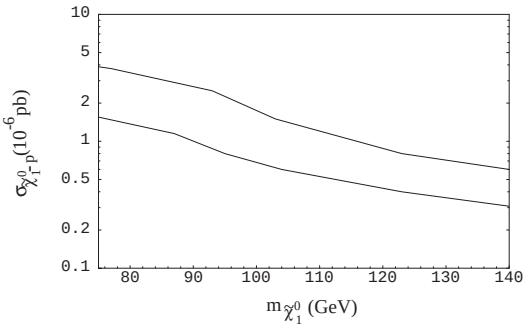

Figure 9. Maximum $\sigma_{\tilde{\chi}_1^0-p}$ for nonuniversal model for $\mu > 0$ with δ_3, δ_4, $\delta_1 < 0$, $\delta_2 > 0$. Lower curve is for $\tan\beta = 7$ and the upper curve is for $\tan\beta = 12$.

For $\mu < 0$, one can again get a cancelation reducing the cross sections below 1×10^{-10} pb for $m_{1/2} > 450$ GeV. As in mSUGRA these can produce sharp minima in the cross sections in the region $\tan\beta$ =10-25.

5 D-Brane Models

Recent advances in string theory has stimulated again the building of string inspired models. We consider here models based on Type IIB orientifolds where the full $D = 10$ space was compactified on a six torus T^6 [3]. These models can contain 9-branes and 5-branes which can be used to embed the Standard Model. We consider here a model in which $SU(3)_C \times U(1)_Y$ is associated with one set of 5-branes, 5_1 and $SU(2)_L$ is associated with a second intersecting set 5_2 [4]. Strings beginning and ending on 5_1 will have massless modes carrying the $SU(3)_C \times U(1)_Y$ quantum numbers (i.e. the R quarks and R leptons), while strings starting on 5_2 and ending on 5_1 will have massless modes carrying the joint quantum numbers of the two branes (i.e. the quark, lepton and Higgs doublets). This then leads to the following soft breaking pattern at M_G:

$$\tilde{m}_1 = \tilde{m}_3 = -A_0 = \sqrt{3}\cos\theta_b \Theta_1 e^{-i\alpha_1} m_{3/2} \qquad (14)$$
$$\tilde{m}_2 = \sqrt{3}\cos\theta_b (1 - \Theta_1^2)^{1/2} m_{3/2}$$

where and $\tilde{m}_i$ are the gaugino masses, and

$$m_{12}^2 = (1 - 3/2\sin^2\theta_b) m_{3/2}^2 \text{ for } q_L,\, l_L,\, H_1,\, H_2 \qquad (15)$$
$$m_1^2 = (1 - 3\sin^2\theta_b) m_{3/2}^2 \text{ for } u_R,\, d_R,\, e_R.$$

Thus the $SU(2)$ doublets are all degenerate at M_G but are different from the singlets. We note Eq. (15) implies θ_b <0.615

This model was initially studied to examine its CP violating properties. However, it was subsequently seen that the experimental constraint of the electron electric dipole moment led to a serious fine tuning problem at M_G unless $\tan\beta \lesssim 3-5$ [28]. Since we are interested here in larger $\tan\beta$, we will set the CP violating phases to zero.

In general, Eq (15) shows that $\sigma_{\tilde{\chi}_1^0-p}$ is an increasing function of θ_b since the squark and slepton masses decrease with increasing θ_b. Thus the maximum cross sections will arise from large θ_b and large $\tan\beta$. This is illustrated in Fig. 10, where $\sigma_{\tilde{\chi}_1^0-p}$ is plotted as a function of $m_{\tilde{\chi}_1^0}$ for $\mu > 0$ for $\tan\beta$ =20, and $\theta_b = 0.2$. Thus we see that current detectors obeying the bound of Eq. (1) are sampling the parameter space for

$$\tan\beta \gtrsim 20 \tag{16}$$

We note that when $\tan\beta$ is close to its minimum value, $m_{\tilde{\chi}_1^0}$ is also close to it's current LEP bound of $m_{\tilde{\chi}_1^0}$ >37 GeV [29,30]. The minimum value of $\sigma_{\tilde{\chi}_1^0-p}$

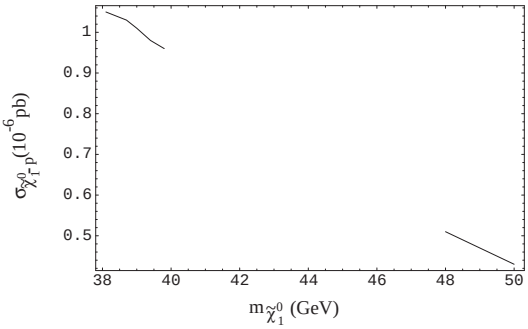

Figure 10. $\sigma_{\tilde{\chi}_1^0-p}$ for D-brane model for $\mu > 0$, $\theta_b = 0.2$ and $\tan\beta = 20$. The gap in the curve is due to excessive early universe annihilation through s-channel Z and h poles.

will occur at low θ_b, low $\tan\beta$, and large $m_{3/2}$ (i.e. large $m_{\tilde{\chi}_1^0}$). In the large $m_{\tilde{\chi}_1^0}$ region, coannihilation can occur between the sleptons and the neutralino in a fashion similar to the SUGRA models, with the effective slepton m_0 parameter and effective neutralino $m_{1/2}$ parameter being given by

$$\begin{aligned} m_0^2 &= (1 - 3\sin^2\,\theta_b)\, m_{3/2}^2 \\ m_{1/2} &= \sqrt{3}\,\cos\theta_b\,\Theta_1\, m_{3/2} \end{aligned} \tag{17}$$

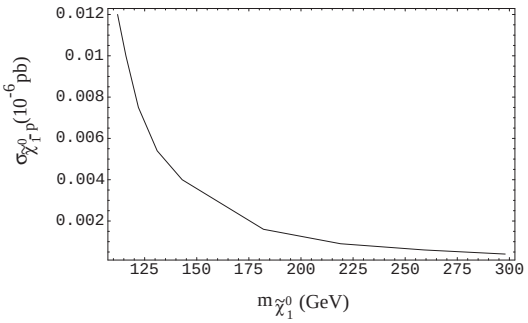

Figure 11. Minimum $\sigma_{\tilde{\chi}_1^0-p}$ for the D-brane model for $\mu < 0$ and $\tan\beta = 6$.

Fig. 11 exhibits the minimum cross section for $\mu > 0$ as a function of the neutralino mass. One sees that

$$\sigma_{\tilde{\chi}_1^0-p} \gtrsim 1 \times 10^{-9} \text{ pb for } \mu > 0 \tag{18}$$

which is accessible to planned detectors. We note also that coannihilation is possible between the light chargino and neutralino. However, this occurs for only a very small region of parameter space.

As in mSUGRA, a cancellation of matrix elements can occur for $\mu < 0$, allowing for the cross sections to fall below the sensitivities of planned future detectors. This is exhibited in Fig. 12, where $\sigma_{\tilde{\chi}_1^0-p}$ is plotted for $\tan\beta = 6$ (solid curve), 12 (dot-dash curve), and 20 (dashed curve). (The $\tan\beta = 6$ curve terminates at low $m_{\tilde{\chi}_1^0}$ due to the m_h constraint, while the higher $\tan\beta$ curves terminate at low $m_{\tilde{\chi}_1^0}$ due to the $b \to s\gamma$ constraint. The upper bound on $m_{\tilde{\chi}_1^0}$, corresponding to $m_{\tilde{g}}$ <1 TeV, arises from the Ωh^2 constraint.) One sees that the cross section goes through a minimum at $\tan\beta \cong 12$, though the expected rise at higher $m_{\tilde{\chi}_1^0}$ does not appear since the parameter space terminates before this sets in.

6 Conclusions

We have examined here the neutralino proton cross section for a number of models possesing grand unification of the gauge coupling constants at $M_G \cong 2 \times 10^{16}$ GeV. The mSUGRA model possesses universal supersymmetry soft breaking masses. In the nonuniversal models, this universality is maintained for the first two generations of squarks and sleptons and for the

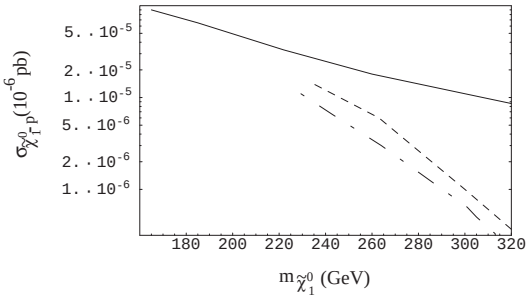

Figure 12. $\sigma_{\tilde{\chi}_1^0-p}$ for the D-brane model for $\mu < 0$ and $\tan\beta = 6$ (solid), $\tan\beta = 12$ (dot-dash), and $\tan\beta = 15$ (dashed).

gaugino masses, but relaxed for the third generation and the Higgs scalar masses. In the D-brane models, universality is violated for both squark and slepton masses at M_G as well as for gaugino masses. Thus each model has a different pattern of soft breaking. Our analysis here also includes the recent experimental bounds on the Higgs mass of $m_h > 114$ GeV [17] (which for GUT models holds for all $\tan\beta$), and the recent theoretical determination of the large $\tan\beta$ corrections to the NLO $b \to s\gamma$ decay [7,8], both of which produce significant effects on limiting the SUSY parameter space. Despite the physical differences between the different models, the general picture resulting is somewhat similar. Thus current detectors obeying Eq(1) are sensitive to significant parts of the parameter space. For mSUGRA they are sampling the regions where $\tan\beta \gtrsim 25$. The nonuniversal models can have cross sections a factor of 10 or larger (with an appropriate choice of nonuniversalities) and so can sample the parameter space with $\tan\beta \gtrsim 7$. The D-brane models require $\tan\beta \gtrsim 20$.

Coannihilation effects play a crucial role for large $m_{\tilde{\chi}_1^0}$ in all the models, and for large $\tan\beta$, they are sensitive to the value of A_0. Large A_0 leads to coannihilation corridors where m_0 can get quite large, thus lowering the value of the $\sigma_{\tilde{\chi}_1^0-p}$ cross section. For $\mu > 0$, the cross sections will generally still be accessible to planned future detectors obeying Eq. (2), i.e.

$$\sigma_{\tilde{\chi}_1^0-p} \gtrsim 1 \times 10^{-10} \text{ pb for } m_{1/2} < 1\,\text{TeV},\ \mu > 0 \tag{19}$$

However, in all models, a special cancellation of the Higgs amplitudes can occur for $\mu < 0$ allowing the cross section to fall below the above bound when $m_{1/2} \gtrsim 450$ GeV. For mSUGRA, these cancellations produce minima where

the cross section essentially vanishes for a range of $m_{1/2}$ when $8 \lesssim \tan\beta \lesssim 30$, for $m_{1/2} < 1$ TeV (see Fig.7) with similar results holding for the nonuniversal models. The cancellations for the D-brane models occur for $10 \lesssim \tan\beta \lesssim 15$. We note that at fixed $\tan\beta$ the cancellations can occur over a wide range of $m_{1/2}$, e.g. for mSUGRA $\tan\beta = 10$, $\sigma_{\tilde{\chi}_1^0 - p} < 10^{-10}$ pb for $400\,\text{GeV} \leq m_{1/2} \leq 1\,\text{TeV}$ [31]. In such regions of parameter space, dark matter detectors would not be able to observe Milky Way dark matter. However, these regions of parameter space would imply that gluinos and squarks lie above 1 TeV, but still should be accessible to the LHC if the parameter space is bounded by $m_{1/2} < 1$ TeV. Thus other experimental consequences of the models would be observable.

References

1. A.H. Chamseddine, R. Arnowitt and P. Nath, *Phys. Rev. Lett.* **49**, 970 (1982); R. Barbieri, S. Ferrara and C.A. Savoy, *Phys. Lett.* B **119**, 343 (1982); L. Hall, J. Lykken and S. Weinberg, *Phys. Rev.* D **27**, 2359 (1983); P. Nath, R. Arnowitt and A.H. Chamseddine, *Nucl. Phys.* B **227**, 121 (1983).
2. For previous analysis of nonuniversal models see: V. Berezinsky, A. Bottino, J. Ellis, N. Fornengo, G. Mignola and S. Scopel, *Astropart. Phys.* **5**, 1 (1996); *Astropart. Phys.* **6**, 333 (1996); P. Nath and R. Arnowitt, *Phys. Rev.* D **56**, 2820 (1997); R. Arnowitt and P. Nath, *Phys. Lett.* B **437**, 344 (1998); A. Bottino, F. Donato, N. Fornengo and S. Scopel, *Phys. Rev.* D **59**, 095004 (1999); R. Arnowitt and P. Nath, *Phys. Rev.* D **60**, 044002 (1999).
3. L. Ibanez, C. Munoz and S. Rigolin, *Nucl. Phys.* B **536**, 29 (1998).
4. M. Brhlik, L. Everett, G. Kane and J. Lykken, *Phys. Rev.* D **62**, 035005 (2000).
5. While the lower bound of Eq.(13) is somewhat lower than other estimates, it allows us to consider the possibility that not all the dark matter are neutralinos, i.e. the dark matter might be a mix of neutralinos, machos, axions etc. Further, the minimum values of $\sigma_{\tilde{\chi}_1^0 - p}$ are not particularly sensitive to the lower bound $\Omega_{\tilde{\chi}_1^0} h^2$.
6. M. Fukugita,hep-ph/0012214.
7. G. Degrassi, P. Gambino and G. Giudice, hep-ph/0009337
8. M. Carena, D. Garcia, U. Nierste and C. Wagner, hep-ph/0010003
9. A. Bottino et al. in ref.[2].
10. A. Bottino, F. Donato, N. Fornengo and S. Scopel, *Astropart. Phys.* **13**,

215 (2000).
11. J. Ellis, T. Falk, K.A. Olive and M. Srednicki, *Astropart. Phys.* **13**, 181 (2000).
12. J. Ellis, A. Ferstl and K.A. Olive, *Phys. Lett.* B **481**, 304 (2000).
13. J. Ellis, T. Falk, G. Ganis and K.A. Olive, *Phys. Rev.* D **62**, 075010 (2000).
14. E. Accomando, R. Arnowitt, B. Dutta and Y. Santoso, *Nucl. Phys.* B **585**, 124 (2000).
15. R. Arnowitt, B. Dutta and Y. Santoso, hep-ph/0005154.
16. J. Ellis, G. Ganis, D. Nanopoulos and K. Olive, hep-ph/0009355.
17. L3 Collaboration (M. Acciarri et al.). CERN-EP-2000-140, hep-ex/0011043; ALEPH Collaboration (R. Barate et al.). CERN-EP-2000-138, hep-ex/0011045.
18. P. Igo-Kemenes, talk presented at ICHEP 2000, Osaka, Japan, July 27-August 2, 2000.
19. I. Trigger, OPAL Collaboration, talk presented at the DPF 2000, Columbus, OH; T. Alderweireld, DELPHI Collaboration, talk presented at the DPF 2000, Columbus, OH.
20. M. Alam et al., *Phys. Rev. Lett.* **74**, 2885 (1995).
21. D0 Collaboration, *Phys. Rev. Lett.* **83**, 4937 (1999).
22. J. Ellis and R. Flores, *Phys. Lett.* B **263**, 259 (1991); *Phys. Lett.* B **300**, 175 (1993).
23. H. Leutwyler, *Phys. Lett.* B **374**, 163 (1996).
24. M. Ollson, hep-ph/0001203.
25. M. Pavan, R. Arndt, I. Stravkovsky, and R. Workman, nucl-th/9912034, *Proc. of 8th International Symposium on Meson-Nucleon Physics and Structure of Nucleon*, Zuoz, Switzerland, Aug., (1999).
26. J. Gasser and M. Sainio, hep-ph/0002283.
27. R. Arnowitt, B. Dutta and Y. Santoso, hep-ph/0010244.
28. E. Accomando, R. Arnowitt and B. Dutta, *Phys. Rev.* D **61**, 075010 (2000)
29. ALEPH Collaboration (R. Barate et al), hep-ex/0011047.
30. The above LEP bound is model dependent and holds for the MSSM. We have checked, however, that it still applies for the D-brane model.
31. We have considered here only the spin independent cross section. As discussed in [32], when the above cancelation is almost complete, the true lower bound on $\sigma_{\tilde{\chi}_1^0-p}$ would be set by the spin dependent part of the cross section. Precisely when this would occur depends on the nuclei used in the target detector.
32. V. Bednyakov and H. Klapdor-Kleingrothaus, hep-ph/0011233.